Journal of Applied Polymer Science

Morphological Correlations to Mechanical Performance of Hydroxyapatite-Filled HDPE/UHMWPE Composites

Harjeet S. Jaggi,[1] Sunil Kumar,[1] Dibyendu Das,[1] Bhabani K. Satapathy,[1] Alok R. Ray[2]
[1]Centre for Polymer Science and Engineering, Indian Institute of Technology Delhi, Hauz Khas, New Delhi 110016, India
[2]Centre for Biomedical Engineering, Indian Institute of Technology Delhi, Hauz Khas, New Delhi 110016, India
Correspondence to: B. K. Satapathy (E-mail: bhabaniks@gmail.com or bhabani@polymers.iitd.ernet.in)

ABSTRACT: Melt mixed and injection molded hydroxyapatite (Hap) filled high-density polyethylene/ultrahigh molecular weight polyethylene composites were assessed for their thermal, structural, morphological, and mechanical attributes. Differential scanning calorimetry was conducted to analyze the effect of Hap loading on various thermal transitions and their associated enthalpies. The microstructural attributes were characterized by conducting wide angle X-ray diffraction and scanning electron microscopy (SEM) of cryo-fractured surface. SEM micrographs of tensile fractured surface revealed the systematic reduction in the size of microfibrils indicating the suppression of local deformation. Improvement in low-strain mechanical response and flexural properties accompanied with a consistent decrease in strain-at-break and toughness was witnessed with increasing Hap content. Toughness aspects were critically discussed in the realms of quasi-static, dynamic mechanical and sudden impact testing approach. Dynamic mechanical analysis demonstrated the presence of prominent α and γ transitions in the crystalline and amorphous phase respectively. Tensile fractured surface morphologies of the investigated composites revealed a switch-over from matrix dominated plastic deformation to Hap controlled quasi-brittle fracture. Thus, our study fundamentally deals with the feasibility of designing polyethylene/Hap composites with superior mechanical properties for biomedical applications, especially for orthopedic implants. © 2014 Wiley Periodicals, Inc. J. Appl. Polym. Sci. **2015**, *132*, 41251.

KEYWORDS: biomedical applications; mechanical properties; morphology; polyolefins

Received 24 April 2014; accepted 2 July 2014
DOI: 10.1002/app.41251

INTRODUCTION

Designing composites based on polyethylene/hydroxyapatite (PE/Hap) as matrix-filler combination with optimal mechanical properties has always been of key interest for materials scientists from biomedical application point of view.[1–5] Factors such as nature of polyethylene matrix, biocompatible/osteocompatible filler content, matrix-filler interfacial adhesion, dimensionality, and size-scale of fillers are of prime concern in meeting a set of mechanical property requirements and optimization.[1,2] The effects of types of biocompatible fillers (hydroxyapatite, tri-calcium phosphate, and β-tri-calcium phosphate) and filler loading on the mechanical properties of high-density polyethylene (HDPE) matrix has been well documented recently, which revealed an improvement in low strain mechanical response (modulus and yield strength) at the cost of reduction in toughness and strain-at-break.[3–5] For example, Jaggi et al.[3] reported the enhancement in tensile modulus (~27%) accompanied by a significant reduction (~33%) in impact strength with 25 wt.% of Hap loading in HDPE matrix. Reduction in the toughness was reportedly attributed to Hap-induced crystallization (nucleation effect) of HDPE matrix. In another independent study, Albano et al.[4] reported the mechanical performance of HDPE/Hap composites with or without ethylene-acrylic acid copolymer as a compatibilizer. Increase in the elastic modulus by ~37% was accomplished along with a significant drop (~99%) in elongation at break, which eventually indicated the transition from ductile to brittle failure for such composite system. Composites fabrication based on silane-treated Hap and acrylic acid grafted HDPE facilitated the penetration of polymer on the Hap particles, thereby leading to enhanced mechanical interlocking as compared with unmodified HDPE/Hap composites.[5] Furthermore, HDPE/Hap composites could not accomplish simultaneous improvement in stiffness and toughness despite interfacial modifications. These findings eventually indicated that the stiffening of HDPE matrix with Hap filler could lead to brittleness of the composite in terms of reduction in impact toughness and strain-at-break.

In an effort to overcome such mechanical properties optimization problems, HDPE was blended with UHMWPE to achieve enhanced toughness without much affecting the stiffness, which

Table I. Raw Materials Specifications

Raw materials	Grade	Supplier	Characteristics
High-density polyethylene	HD50MA180	Reliance Industries Limited	Density (ρ) = 0.95 g/mL; MFI (g/10 min) = 20 @ 190°C, 2.16 kg
Ultra high molecular weight polyethylene	M4	Bhilwara Polymers	Density (ρ) = 0.932 g/mL; $M_w = 443 \times 10^4$
Hydroxyapatite	Ossein	Clarion Pharmaceutical Co. Gurgaon	Particle density = 3.14 g/cc; hardness 5 Mohs scale; particle size in micron

is further expected due to superior crack resistance behavior of UHMWPE and its compatibility to HDPE because of similar chemical structure. In this regard, numerous researchers have documented the mechanical performance vis-à-vis processability aspects of HDPE/UHMWPE blends in the recent decade.[6–10] Lim et al.[6] reported the melt mixing of such blend system by using Brabender torque rheometer and further optimized the 50 : 50 (w/w) blend composition in terms of processability and mechanical properties. Lucas et al.[7] investigated the wear and mechanical performance of extrusion melt-mixed HDPE/UHMWPE blend with varied concentration (10–30 wt %) of UHMWPE. Improvement in the tensile, impact, and wear resistance properties were registered with increasing UHMWPE content. Our recent work based on rheological, morphological and mechanical response correlations of HDPE/UHMWPE blend system has clearly demonstrated simultaneous increase in the stiffness and toughness with increasing UHMWPE content.[8] These improvements in tensile and impact properties were further attributed to the enhanced crystallinity of formulated blend and better energy absorbing capacity of dispersed UHMWPE phase respectively.[8] Recently, Xu et al.[9] reported the structural changes induced mechanical response of HDPE/UHMWPE blends using oscillatory shear injection molding (OSIM). Significant improvement in the tensile and impact properties was reported with increasing UHMWPE content in the blend matrix. Such an observation in terms of improved mechanical properties was reportedly attributed to the more pronounced molecular orientation caused by amplifying flow velocity between HDPE and UHMWPE phases. These findings from literature eventually lead to an understanding that the blending of HDPE with UHMWPE could lead to simultaneous improvement in stiffness and toughness unlike HDPE/Hap composites.

Interestingly, the influence of UHMWPE incorporation on the mechanical properties of HDPE/$CaCO_3$ composites was investigated by Suwanprateeb.[11] Improvement in the strain-at-break and Izod impact strength was observed with increasing UHMWPE content in HDPE/UHMWPE/$CaCO_3$ composites, which further indicated the improved ductility of such ternary composite system. Such an improvement in impact toughness was reportedly attributed to the enhanced crack propagation resistance and good energy absorbing capacity of UHMWPE particles. Furthermore, mechanical performance of nano β-tricalcium phosphate reinforced HDPE/UHMWPE nanocomposites was investigated by Abadi et al.,[12] which revealed an improvement in tensile modulus and yield strength accompanied by a slight reduction in yield strain with nanofiller incorporation. These observations in terms of improved tensile and impact properties due to UHMWPE incorporation need

Table II. Composition and Designation of HDPE/UHMWPE/Hap Composites

Composite composition	HDPE/UHMWPE[a] (wt %)	Hydroxyapatite (wt %)
HUH0	100	0
HUH5	95	5
HUH10	90	10
HUH15	85	15
HUH20	80	20
HUH25	75	25

[a] Represents optimized blend matrix i.e., (HDPE : UHMWPE) in 70 : 30 ratio.

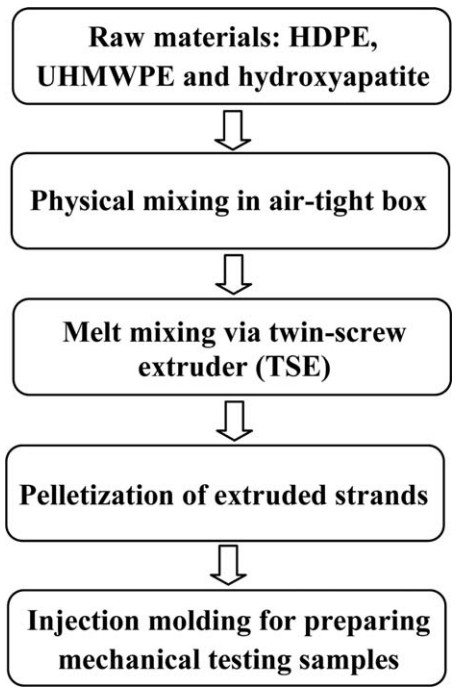

Figure 1. Flow-diagram showing the composites fabrication process.

Table III. (A) Extruder Temperature (°C) Profile (B) Temperature Profile Set in Injection Molding Machine (C) Processing Conditions Used in Injection Molding

(A)							
Zones	Z-1	Z-2	Z-3	Z-4	Z-5	Z-6	Z-7
Temp. (°C)	140	150	160	170	180	190	195
(B)							
Zones	Feed	Z-I	Z-II	Z-III	Nozzle		
Temp. (°C)	40	150	165	180	195		
(C)							
Process parameter	Value						
Injection pressure	60–70% (bars)						
Injection speed	45%						
Holding time	5 s						
Cooling time	25 s						

detailed analysis with emphasizing on the toughness aspects of such particulate filled ternary composites. Additionally, over the years PE-Hap biocomposites has gained preference as potential structural matrix for various biomedical applications. Interestingly, orthopedic implants as an alternative to bone analogs required low modulus and high tensile strength. For example, cancellous bone has modulus and tensile strength of 0.4 GPa and 7.4 MPa, respectively.[13] The modulus mismatch between bone and metallic or ceramic implants has been of major concern in orthopedic surgery; which may lead to stress shielding i.e., insufficient load borne by the bones and hence affect the remodeling and healing process of the bone tissue.[13,14] On the other hand, the low modulus of polymeric materials makes it a promising candidate for such applications; though, the low tensile strength limits its potential use. However, incorporation of micro/nano fillers in the polymer matrix may enhance the tensile strength substantially. Furthermore, merit of such biocomposites is that by controlling the filler concentration, the properties can be varied and easily tailor-made to suit the mechanical properties of host tissue.[13]

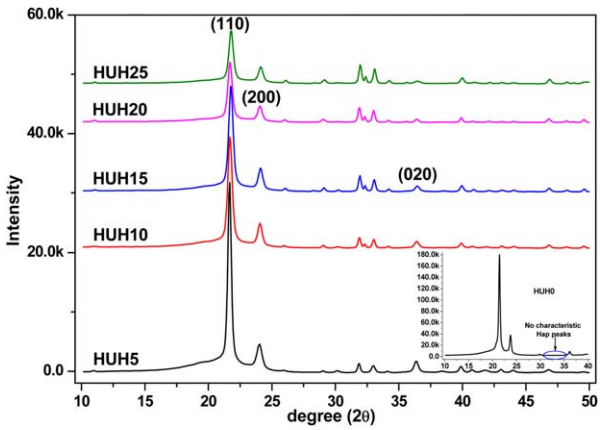

Figure 2. X-ray diffractograms of hydroxyapatite-filled composites. [Color figure can be viewed in the online issue, which is available at wileyonlinelibrary.com.]

Incorporation of Hap introduces rigidity to the HDPE matrix, which in turn brings about brittleness in the composites. Although, it could be expected that Hap incorporation to the HDPE/UHMWPE matrix will not deteriorate the toughening efficiency to a large extent unlike HDPE/Hap composites. Thus, our study fundamentally deals with the improvement in low strain mechanical response without much affecting the toughening efficiency of the HDPE/UHMWPE/Hap composites. It further takes a closer look into the structural, morphological, quasi-static, and dynamic mechanical response of Hap-filled HDPE/UHMWPE composites and explores the possible correlations amongst them.

EXPERIMENTAL

Fabrication of HDPE/UHMWPE/Hap Composites

Blending of HDPE, UHMWPE and hydroxyapatite is done firstly by physical mixing in an airtight box. Table I shows the details of raw materials used in this study. Melt mixing of the formulated composition is performed in a corotating type twin-screw extruder (Model L/D 40, Steer Omega-20) at a screw speed of 200 rpm. The details of the composites formulation and their designation are presented in Table II. Polymer strands (obtained from TSE) were later chopped in a dry strand pelletizer from Glaves Corporation Pvt. Ltd. The chopped granules were subsequently kept for drying in an oven prior to injection molding (L & T Demag PFY-40). The flow-diagram showing the composite fabrication process is presented in Figure 1. The processing conditions of extrusion and injection molding process are shown in Table III.

Structural Characterization

Wide Angle X-ray Diffraction. Wide angle X-ray diffraction (WAXD) was carried out on injection molded test specimens to characterize the peak intensity and/or shift in the peaks corresponding to different crystal planes. The WAXD measurements were performed on a X-ray diffractometer from Philips X'Pert-PRO, PANalytical diffractometer using Cu K_α radiation ($\lambda = 1.54$ Å) in the radial scattering range of $2\theta \sim 10$–40°. The sample to detector distance was kept constant at 120 mm.

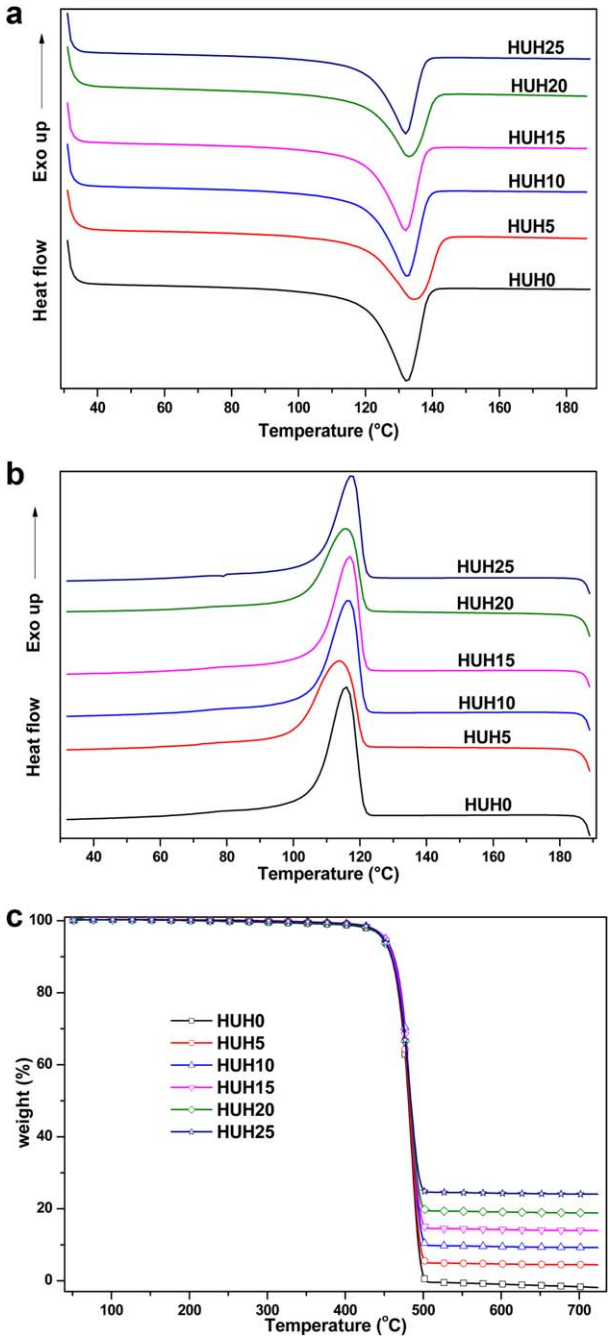

Figure 3. (a) DSC melting endotherm (b) Cooling exotherm (c) TGA traces of filled composites. [Color figure can be viewed in the online issue, which is available at wileyonlinelibrary.com.]

Thermal Characterization

Differential scanning calorimetry (Q200, TA Instruments, USA) was carried out to analyze the various thermal transitions involved during heating and cooling processes and their associated enthalpies. The fine sized particles were cut from injection moulded testing specimen of the investigated compositions. It was heated from 30°C to 190°C at the rate of 10°C/min under nitrogen atmosphere and then kept at that temperature for 3 min to remove any kind of thermal history. It is then cooled down to room temperature at a rate of 10°C/min for attaining the crystallization temperature and its associated enthalpy. It was again heated till 190°C at the rate of 10°C/min for the assessment of melting transition and its associated enthalpy. First crystallization enthalpy, second melting enthalpy, and their corresponding thermal transitions were used for analysis in this study.

Eventually, the percentage crystallinity was calculated using the following eq. (1).

$$X_c = \frac{\Delta H_m}{\Delta H_{\mathrm{mo}} \times (1-w)} \times 100 \quad (1)$$

where, ΔH_m is the melting enthalpy of investigated compositions and ΔH_{mo} is the melting enthalpy of 100% crystalline polyethylene, which is taken as 292 J/g.[15] The wt. fraction of filler in the composite is denoted by w.

Thermogravimetric analysis (Pyris 6 TGA; Perkin-Elmer Pvt. Ltd.) was carried out to study the thermal stability in terms of shift in the onset to degradation temperature. The experiments were performed at a heating rate of 20°C/min under nitrogen atmosphere in the temperature range of 50–720°C.

Measurement of Mechanical Properties

Zwick Z250 universal testing machine was used for uni-axial tensile testing conforming to ASTM D638 test standard with a crosshead speed of 20 mm/min. Flexural properties such as flexural strength and modulus were measured on a Zwick Z010 testing machine following ASTM D790 method in a three point bending mode. Tinius-Olsen impact tester was used to measure the notched Izod impact strength of the investigated composites following ASTM D256 test standard.[16]

Dynamic Mechanical Analysis

Dynamic mechanical analyzer (Q800; TA Instruments, USA) was used to characterize the viscous and elastic response of filled composites in a single cantilever mode. Testing specimens of dimension 35 × 13 × 3 mm^3 were cut from injection molded rectangular bars. DMA test was performed at a constant frequency of 1 rad/s. The temperature was varied from −125°C to 105°C at a heating rate of 5 K/min.

Fractured Surface Morphology

The cryogenically fractured surface morphologies of filled composites have been investigated by using scanning electron microscopy (SEM) on a Zeiss EVO 50 apparatus to study the dispersed phase (UHMWPE) morphology and the distribution/dispersion state of Hap fillers. SEM of the tensile fractured surface morphologies has been analyzed to understand the associated failure mechanism. Gold sputter coating of fractured samples is done prior to examination to make the surface conductive.

RESULTS AND DISCUSSION

Structural and Thermal Characterization

The structural interpretations of hydroxyapatite filled HDPE/UHMWPE composites have been made from WAXD on injection molded testing specimen. Figure 2 shows the XRD plots of optimized blend matrix (see inset) and Hap filled composites in terms

Table IV. DSC/TGA Data of Optimized Blend and HDPE/UHMWPE/Hap Composites

	DSC				TGA		
	Melting endotherm			Cooling exotherm			
Composite designation	T_{onset} (°C)	T_m (°C)	Crystallinity (%)	T_c (°C)	T_{onset} (5 wt % loss) (°C)	T_{onset} (10 wt % loss) (°C)	T_{max} (°C)
HUH0	120.72	131.36	68.25	116.01	447.33	459.62	477.87
HUH5	120.71	134.35	60.23	113.72	448.82	459.61	478.91
HUH10	121.58	132.48	69.86	116.58	452.49	462.60	479.95
HUH15	120.96	131.94	69.09	116.88	450.43	460.65	479.94
HUH20	121.65	132.90	64.81	115.82	449.39	459.61	478.91
HUH25	121.49	132.07	69.86	117.50	449.39	458.58	479.94

of intensity versus 2θ measured in the range of 10–40°. The blend matrix is characterized by the appearance of sharp and intense polyethylene peaks at 2θ angles of ~ 21.4° and ~23.7° corresponding to (110) and (200) orthorhombic crystal planes, respectively.[17] A less intense PE shoulder peak was also obtained at an angle of $2\theta \sim 36.2°$ corresponding to (020) plane. On the other hand, filled composites at different concentrations are characterized by the appearance of relatively less intense Hap peaks corresponding to 2θ angles of ~31.9° and ~33.1°. Additionally, reduction in the intensity of characteristic polyethylene peaks along with a gradual increase in Hap peak intensity was registered with increasing Hap concentration in filled composites. Interestingly, the appearance of distinct characteristic peaks corresponding to the matrix (polyethylene phase) and filler (Hap) clearly revealed the noninterference of crystal planes indicating no chemical or phase transformation interactions.

Figure 3(a,b) presents the melting and cooling thermograms of the investigated composites. Melt mixing of HDPE/UHMWPE/Hap composites has caused broadening of the cooling and melting peaks, which eventually indicated the possibility of a slightly broader crystallite size distribution with increasing Hap content. This may further be attributed to Hap-induced mobility restriction of polyethylene matrix. Thermal transitions such as melting and crystallization temperatures (T_m and T_c) were found to be remained unaffected barring the composite HUH5, which showed slightly higher melting temperature (~3°) along with decrease in crystallization temperature (~3°) as evident from Table IV. TGA studies have revealed unaffected thermal stability of blend matrix due to Hap incorporation as evident from Figure 3(c). The degradation temperatures at 5 and 10 wt % loss and temperature at maximum weight loss rate (T_{max}) are presented in Table IV. In general, the degradation temperatures were found to be broadly unaffected with increasing Hap content in the blend matrix, which further indicated the absence of any structural interaction in filled composites. Hydroxyapatite was found to be thermally stable till the maximum temperature of 720°C as evident from the TGA thermograms [Figure 3(c)]. Percentage char obtained after complete degradation of polyethylene matrix as shown in TGA plot (>510°C) confirms the weight percentage of Hap filler in the formulated compositions.

Dynamic Mechanical Properties (DMA)

In this technique, an oscillating force is applied to the testing specimens. A phase difference between the applied stress and resulting deformation has been obtained as shown in the following equation.[18]

$$\varepsilon = \varepsilon_0 \sin(\omega t) \quad (2)$$

$$\sigma = \sigma_0 \sin(\omega t + \delta) \quad (3)$$

where, ω, t, and δ are frequency of oscillation, time, and phase difference respectively, whereas σ_0 and ε_0 are the maximum stress and its corresponding strain. After expansion eq. (3) becomes

$$\sigma = \sigma_0 \sin(\omega t) \cos\delta + \sigma_0 \cos(\omega t) \sin\delta \quad (4)$$

Stress is eventually divided by strain to separate the modulus into one in-phase and another out-of-phase component with strain. These in-phase and out-phase components are also referred as storage and loss modulus (E' and E'') and are responsible for storing energy elastically and as heat dissipation respectively. Thus, the stress strain relationship can further be written as:

$$\sigma = \varepsilon_0 E' \sin(\omega t) + \varepsilon_0 E'' \cos(\omega t) \quad (5)$$

$$E' = \sigma_0 \cos\delta / \varepsilon_0 \quad (6)$$

$$E'' = \sigma_0 \sin\delta / \varepsilon_0 \quad (7)$$

Composition specific storage and loss moduli (E' and E'') as a function of temperature are shown in Figure 4(a). Reduction in the E' value was observed with increasing temperature, which may be due to thermal movements of the side chain segments caused by increased thermal energy. The DMA plots clearly revealed the increase in storage and loss moduli with increasing filler content. This is further attributed to the enhanced mechanical interlocking caused by the physical interaction between matrix and Hap filler in the composites. Although, this hindrance caused by shrinkage of polymer chain over Hap particles decreases with increasing thermal movements, which further leads to lower extent of increase in storage modulus with increasing temperature. Various thermal transitions in the polyethylene could be referred as α, β, and γ relaxations in the decreasing order of temperature, where α and γ

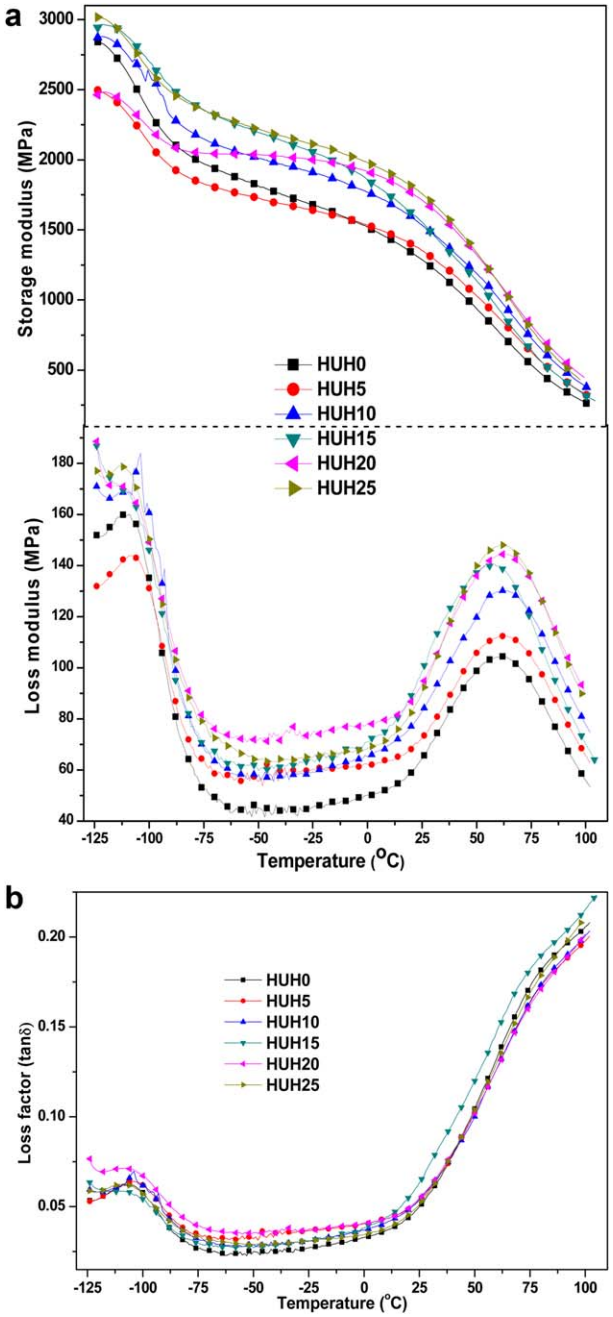

Figure 4. Dynamic mechanical analysis plots of the composites (a) storage and loss moduli and (b) loss factor as a function of temperature. [Color figure can be viewed in the online issue, which is available at wileyonlinelibrary.com.]

are the prominent transitions in the crystalline and amorphous phase respectively as evident from the loss modulus versus temperature plot. Interestingly, the β transition was not found as prominent as α and γ transitions, which is further attributed to the high crystallinity of investigated composite system. A sharp reduction in the E' value was observed in the temperature range of -125°C to -75°C indicating the γ-transition regime, which is due to the relaxation of restricted rotation of small methylene group attached to main chain in the amorphous region as evident from Figure 4(a).[18] The γ-transition regime is followed by a plateau-like weak β-transition in the temperature range of $-75°$ to 10°C, which further indicated the segmental motion of side chain in the interfacial region between crystalline and amorphous phases.[18] The β-region is trailed by a sharp reduction in E' indicating crystal-crystal slippage in α-transition regime as typical in semicrystalline polymers till 105°C.[3] Loss moduli versus temperature plots are typically drawn to characterize the energy dissipation ability of the filled composites. Loss modulus was found to be increased with increasing Hap filler content. Additionally, the loss-peak width gets broadened with filler addition, which further indicated the contribution of higher fraction of polymer chains towards energy dissipation process due to matrix-filler interaction.[18]

Loss tangent as a function of temperature [Figure 4(b)] is typically drawn to study the damping response of HDPE/UHMWPE/Hap composites. In the solid state transition regime (β and γ transitions), the damping parameter was found to be in the range of 0.03–0.07. Significant improvement in the damping properties along with a singularity response (barring HUH15) was observed with further increase in temperature (till 60°C) for the investigated composites. Such an observation in singularity response for polymer blends has recently been reported by Sunil et al., which revealed that the net elastic and inelastic deformation behaviors get compensated in very similar fashion.[19]

Cryo-Fractured Surface Morphology

Scanning electron microscopy (SEM) is carried out to analyze the morphological attributes of cryogenically fractured samples for the better understanding of phase morphology and the dispersion/distribution state of Hap fillers. Figure 5(a–f) depicts the SEM micrographs of optimized blend matrix and Hap-filled HDPE/UHMWPE composites. Interestingly, a two-phase morphology was observed for blend matrix [Figure 5(a)], where UHMWPE phase was found to be dispersed in the HDPE matrix. Such an observation of distinct two-phase morphology along with strong interphase have already been reported for HDPE/UHMWPE blends.[7,20] Hydroxyapatite filler was found to be well dispersed in the blend matrix especially at lower loading. Though, Hap agglomeration could be noticed at higher loading as evident from the Figure 5(e,f). Few of the Hap particles detached from matrix were found over the fractured surface and/or in the cavity. At higher magnification, few Hap particles were found to be highly intact (embedded) within the polymer indicating the good mechanical interlocking. Such an observation of better mechanical interlocking between polymer and reinforcement is well complemented by improved mechanical properties of investigated composite system.

Mechanical Properties Investigations

Tensile and Flexural Properties. The stress-strain response of optimized blend matrix and filled composites is shown in Figure 6. It was observed that the maximum load sustained by composites increases consistently with increasing Hap content accompanied with a linear decrease in strain-at-break. The area under the stress–strain curve was found to be decreased with increasing filler content indicating the Hap induced reduction in toughness. The toughness measurements following various methods viz. notched Izod impact test (sudden loading), area

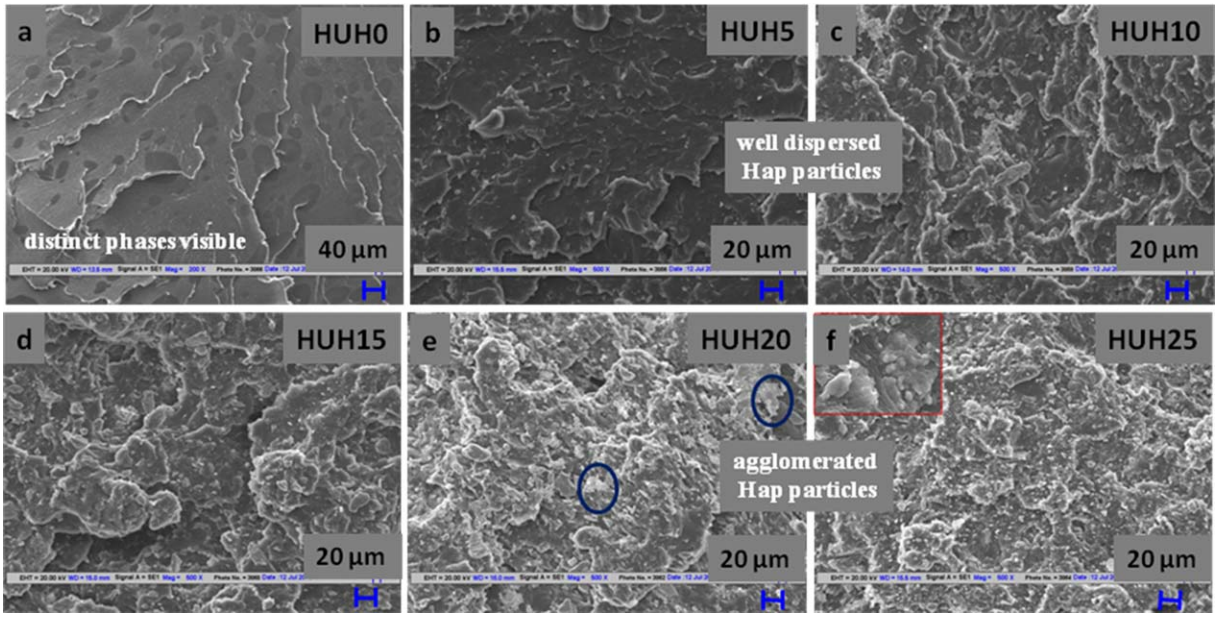

Figure 5. Morphology as observed by scanning electron microscopy (SEM) of the cryo-fractured surfaces of the composites (a) HUH0, (b) HUH5, (c) HUH10, (d) HUH15, (e) HUH20 and (f) HUH25. [Color figure can be viewed in the online issue, which is available at wileyonlinelibrary.com.]

under stress–strain curve (quasi-static tensile testing) and brittleness index (employs both quasi-static as well as dynamic mechanical testing) have been critically discussed in the subsequent section. The variation in stress-at-break (σ_b), strain-at-break (ε_b), Young's modulus (E), and yield strength (σ_y) is shown in Figure 7. Strain-at-break indicating the bulk deformation response has shown a reduction of ~45.3% upon maximum Hap loading. This reduction in the strain-at-break has been found to have a correspondence with local deformation response in terms of reduced microfibril size as obtained from SEM images and has been discussed critically in the later section. Interestingly, tensile yield strength showed a two-stepped jump specifically ~10.6% and ~10.7% in the composition domain of 5–10 wt % and 15–20 wt % of Hap loading respectively, whereas the stress-at-break and Young's modulus showed an increase by ~129% and ~28.7% upon maximum Hap loading. These improvements in the mechanical properties may be attributed to better Hap distribution and other shear induced effects, which may have promoted the transformation of ductility-reduction into strength-enhancements.[3] Although, tensile properties was found to be unaffected in the composition window of 20–25 wt % of Hap content, which further indicated the filler agglomeration at higher Hap content.

The flexural properties of investigated composites as a function of Hap content is shown in Figure 8. The flexural modulus and strength were found to increase to a maximum of ~39.7% and ~38.6% respectively at 20 wt % of Hap loading in the blend

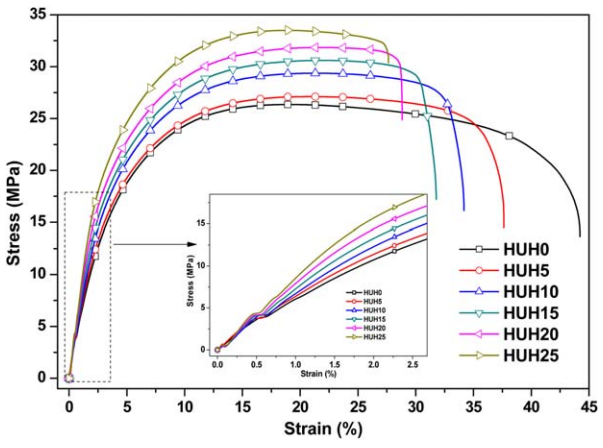

Figure 6. Stress–strain curve of composites as a function of hydroxyapatite content. [Color figure can be viewed in the online issue, which is available at wileyonlinelibrary.com.]

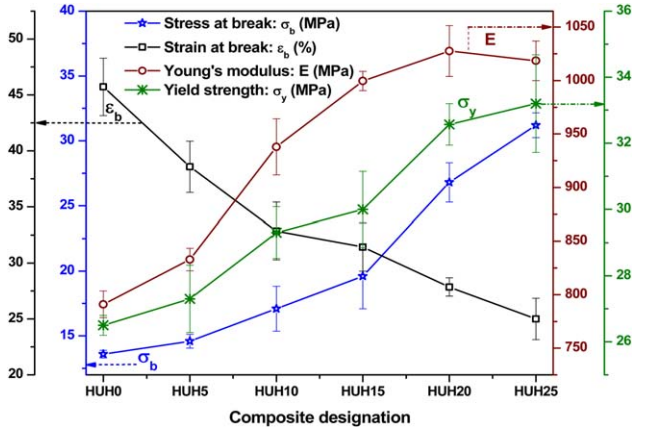

Figure 7. Tensile modulus (E), yield strength (σ_y), Stress-at-break (σ_b), and strain-at-break of the composites as a function of hydroxyapatite content. [Color figure can be viewed in the online issue, which is available at wileyonlinelibrary.com.]

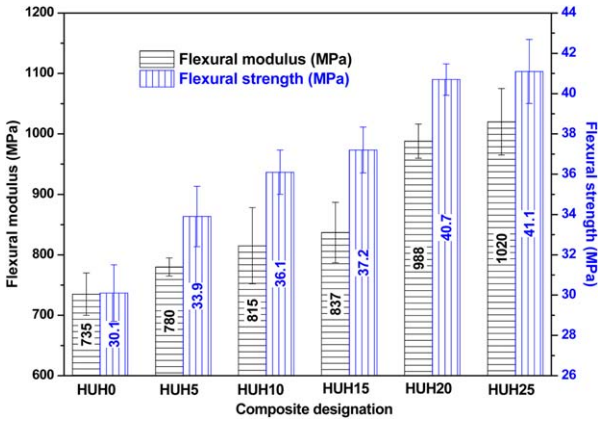

Figure 8. Flexural modulus and flexural strength of the composites as a function of hydroxyapatite content. [Color figure can be viewed in the online issue, which is available at wileyonlinelibrary.com.]

matrix. This increase in the flexural properties may be attributed to the filler induced rigidity (mechanical restraint) to the composite system. Further increase in Hap loading may lead to marginal increase in bending resistance indicating the disperse phase (Hap) agglomeration. Additionally, the degree of crystallinity of the investigated composite system were found to be slightly higher than that of blend matrix barring the composites HUH5 and HUH20, which further led to improvement in flexural properties. Such an observation from flexural testing indicated the possibility of reaching at maximum bending rigidity at 20 wt % of Hap loading in the blend matrix. These findings from mechanical testing revealed the improved tensile and flexural strength along with comparable modulus value with bones; which makes such biocomposites suitable for various biomedical applications, especially in orthopedic applications.

Toughness Assessment. Toughness properties of polymer based blends and composites are of paramount importance for designing prospects as well as from performance point of views. Interestingly, various methods viz. notched Izod impact test, Charpy impact test, tensile test (area under stress–strain curve) and brittleness index (employs both quasi-static and dynamic mechanical tests) are being used for the toughness assessment of such polymer system.[21,22] Izod impact strength is defined as breaking energy (E) per unit of notched specimen thickness (t) i.e., $E.t^{-1}$, whereas Nielsen and Landel defined the toughness as area under stress–strain curve obtained from uni-axial tensile testing.[21] Brostow et al.[22] had validated a semiempirical parameter referred as brittleness index (BI) = $[\varepsilon_b E']^{-1}$; where ε_b is percentage elongation at break and E' is the storage modulus obtained from DMA at a particular temperature and frequency. Brittleness index could practically be considered as more reliable technique for toughness measurement, because the parameter E' takes into account the viscoelastic nature and repetitive loading (fatigue) experienced by polymeric materials during service.[22] On the other hand, ε_b indicates the maximum deformation ability of polymeric materials prior to failure during tensile testing. The variations in brittleness index, notched Izod impact strength and area under stress–strain curve as a function of composition are shown in Figure 9. The storage modulus (E') value was taken at a temperature of 25°C for the assessment of brittleness index. Incorporation of 25 wt % of Hap filler in the optimized blend matrix has led to a decrease of ~34.7% and ~20.8% for Izod impact strength and area under the stress–strain curve respectively accompanied by an increase of ~14.5% in the brittleness index value. Such an observation in toughness reduction may be attributed to the Hap filler induced mechanical restrictions to the polymer chain mobility/bulk matrix deformation. Sewda et al.[23] recently reported the impact strength reduction of filled HDPE composites, which was reportedly attributed to the stress concentration points produced around the filler particles. Furthermore, filler induced crystallization (reduced amorphization) decreases the tendency of energy absorbing capacity, thereby reduces the impact toughness. Though, the reduced impact value even at maximum Hap loading was found to be well above the neat HDPE matrix.[8] In another independent study, Lim et al.[24] reported the mechanical performance of melt mixed (using Brabender Plasticorder) HDPE/Hap and HDPE/UHMWPE/Hap composites, which has revealed better toughness for composites containing HDPE/UHMWPE as base matrix. This was reportedly attributed to the extensive plastic deformation in the form of microfibril formation, which enhanced the toughening efficiency of HDPE/UHMWPE/Hap composites. Eventually, an inverse relation between Izod impact strength and brittleness index was obtained for investigated composites with an appreciable R-square value of 0.936 as shown in the inset of Figure 9. Interestingly, Izod impact strength value was found to be constant at high brittleness indices, which fundamentally indicates that even a very brittle composite could offer some impact resistance. Similar results on the uniform impact strength (Charpy and Izod impact strength values) at high brittleness indices have been reported recently.[25]

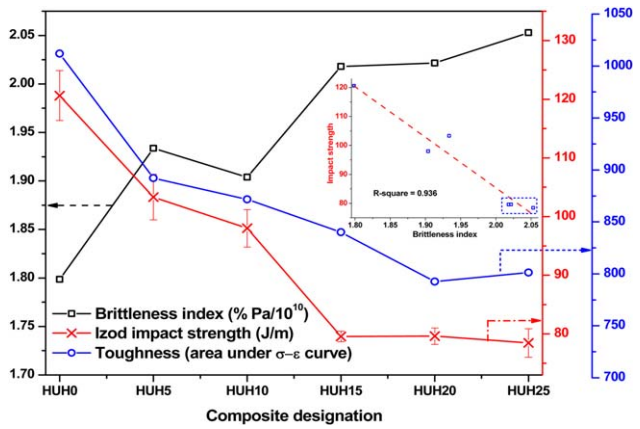

Figure 9. Variation of Izod impact strength, toughness and brittleness as a function of composition. [Color figure can be viewed in the online issue, which is available at wileyonlinelibrary.com.]

Tensile Fractured Surface Morphology

Scanning electron microscopy (SEM) of tensile fractured surface is carried out to study the nature of fractured surface morphology and associated failure mechanism. Figure 10(a–f) depicts the SEM micrographs of optimized blend matrix and Hap-filled HDPE/UHMWPE composites. The blend matrix experienced a

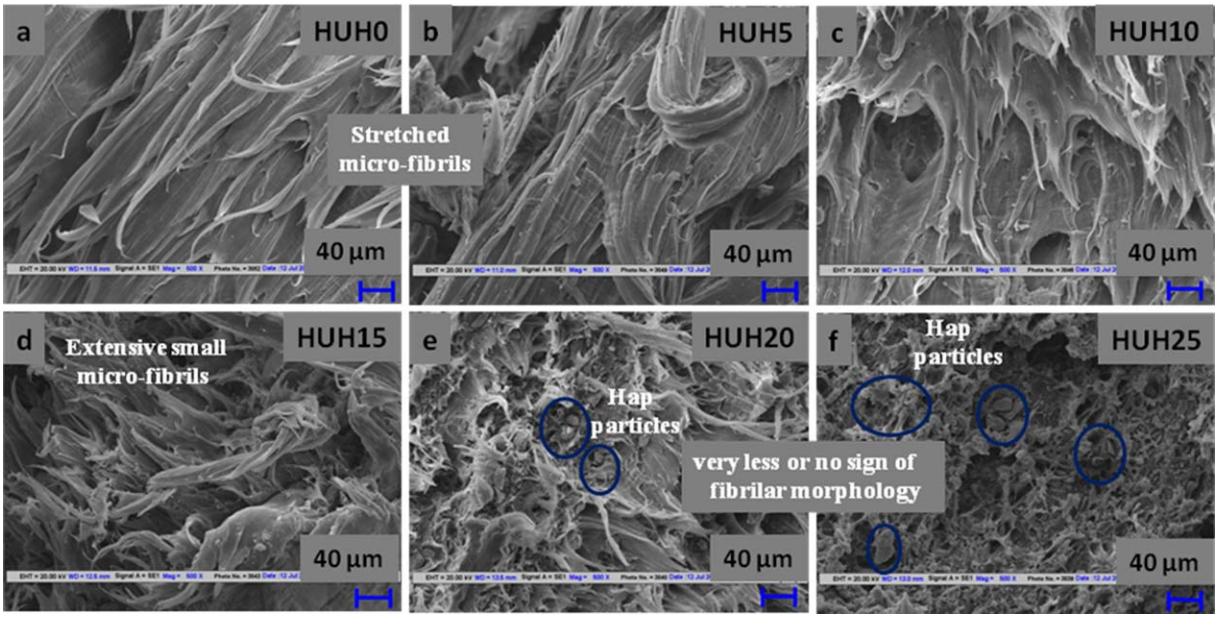

Figure 10. Morphology as observed by scanning electron microscopy (SEM) of the tensile-fractured surfaces of the composites (a) HUH0, (b) HUH5, (c) HUH10, (d) HUH15, (e) HUH20, and (f) HUH25. [Color figure can be viewed in the online issue, which is available at wileyonlinelibrary.com.]

relatively large local deformation, which consistently reduced with increasing Hap loading as evident from SEM images. Interestingly, tensile fractured surface morphologies showed a very systematic change in local deformation mode, which is evident from the transformation of fibrilar morphology from stretched to hindered microfibrils with increasing Hap loading. These findings from morphological attributes have eventually indicated the ductile to brittle transition with increasing filler content. Specifically, the optimized blend matrix and composite with 5 wt % of Hap content undergo ductile failure accompanied with plastic deformation as evident from stretched microfibrils [Figure 10(a,b)]. Further increase in the Hap loading (10–15 wt %) has led to relatively smaller microfibrils indicating ductile to semiductile transition (DST) as evident from Figure 10(c,d). However, further increase in the Hap content to 20–25 wt % has shown hindered microfibrils, which eventually indicated the brittle failure of such composite system at higher Hap loading as observed from Figure 10(e,f). These morphological changes in terms of suppression of local deformation could lead to an understanding of ductile to brittle transition with increasing Hap content, which has found to have a correspondence with transitions in mechanical response in terms of strain-at-break (bulk deformation response) and tensile yield strength (low strain mechanical response) as evident from the Figure 7. These findings from morphological interpretations may be attributed to Hap induced mechanical restrictions to polymer chain mobility; an aspect clearly visible in the bulk mechanical response in terms of reduction in elongation at break with increasing Hap content.

CONCLUSIONS

Hap filled HDPE/UHMWPE composites were fabricated via melt mixing in a twin screw extruder followed by injection molding for the preparation of mechanical testing specimens. Structural characterization using WAXD revealed the noninterference of the crystalline planes of matrix and filler as observed from their distinct characteristic peaks in the investigated composites. DSC analysis revealed inappreciable changes in thermal transitions, whereas the percentage crystallinity did not show a specific trend. Thermal gravimetric analysis revealed that the degradation temperatures remained nearly unaffected despite Hap incorporation indicating the absence of any structural interaction. Dynamic mechanical response demonstrated improvement in storage modulus due to mechanical restraint caused by Hap particles, which however diminishes with increasing temperature due to increased thermal movement. SEM of the cryogenic fractured surface depicts two phase morphology with dispersed UHMWPE phase in HDPE for optimized blend matrix, whereas composites showed uniform distributed/dispersed state (till 15 wt %) of Hap loading. Incorporation of 20 wt % of Hap in the blend matrix has caused an improvement in the tensile properties such as tensile modulus, ultimate tensile strength, and yield strength by ~28.7%, ~129%, and ~25.3% respectively. On the other hand, strain-at-break and notched Izod impact strength decreased by ~45.3% and ~34.7% respectively at maximum Hap loading. Incorporation of Hap in the blend matrix has further caused an improvement in flexural properties such as modulus and strength by ~39.7% and ~38.6% respectively at maximum Hap loading. Interestingly, brittleness index (BI) and Izod impact strength showed an inverse relationship with an appreciable regression coefficient value. Tensile fractured surface morphologies indicated the ductile to brittle transition in the deformation modes via systematic change in the fibrilar morphology from stretched to hindered microfibrils with increasing Hap content. These findings in terms of suppression of local deformation were found to have a correspondence with bulk deformation response in the similar composition window. Thus our study fundamentally demonstrates the feasibility of designing

hydroxyapatite-filled HDPE/UHMWPE composites for biomedical applications showing enhanced tensile and flexural properties without much affecting the toughening efficiency.

ACKNOWLEDGMENTS

Authors gratefully acknowledge the funding support by Department of Biotechnology, Government of India, New Delhi, India, vide the sponsored research project Grant No. BT/PR13299/MED/32/128/2009.

REFERENCES

1. Wang, M.; Joseph, R.; Bonfield, W. *Biomaterials* **1998**, *19*, 2357.
2. Cheang, P.; Khor, K. A. *Mater. Sci. Eng. A* **2003**, *345*, 47.
3. Jaggi, H. S.; Kumar, Y.; Satapathy, B. K.; Ray, A. R.; Patnaik, A. *Mater. Des.* **2012**, *36*, 757.
4. Albano, C.; Perera, R.; Catano, L.; Karam, A.; Gonzalez, G. *J. Mech. Behav. Biomed.* **2011**, *4*, 467.
5. Wang, M.; Bonfield, W. *Biomaterials* **2001**, *22*, 1311.
6. Lim, K. L. K.; Ishak, Z. A. M.; Ishiaku, U. S.; Fuad, A. M. Y.; Yusof, A. H.; Czigany, T. *J. Appl. Polym. Sci.* **2005**, *97*, 413.
7. Lucas, A. d. A.; Ambrósio, J. D.; Otaguro, H.; Costa, L. C.; Agnelli, J. A. M. *Wear*, **2011**, *270*, 576.
8. Jaggi, H. S.; Satapathy, B. K.; Ray, A. R. *J. Polym. Res.* **2014**, *21*, 482. DOI 10.1007/s10965-014-0482-8.
9. Xu, L.; Huang, Y. F.; Xu, J. Z.; Ji, X.; Li, Z. M. *RSC Adv.* **2014**, *4*, 1512.
10. Chen, Y.; Li, Y.; Zou H.; Liang, M. *J. Appl. Polym. Sci.* **2014**, *131*, 39916.
11. Suwanprateeb, J. *J. Appl. Polym. Sci.* **2000**, *75*, 1503.
12. Abadi, M. B. H.; Ghasemi, I.; Khavandi, A.; Shokrgozar, M. A.; Farokhi, M.; Homaeigohar, S. S.; Eslamifar, A. *Polym. Compos.* **2010**, *31*, 1745.
13. Ramakrishna, S.; Mayer, J.; Wintermantel, E.; Leong, K. W. *Compos. Sci. Technol.* **2001**, *61*, 1189.
14. Scholz, M. S.; Blanchfield, J. P.; Bloom, L. D.; Coburn, B. H., Elkington, M.; Fuller, J. D.; Gilbert, M. E.; Muflahi, S. A.; Pernice, M. F.; Rae, S. I.; Trevarthen, J. A.; White, S. C.; Weaver, P. M.; Bond, I. P. *Compos. Sci. Technol.* **2011**, *71*, 1791.
15. Wundelrich, B. Macromolecular Physics: Crystal Melting, Vol. *3*, Academic Press: New York, **1980**.
16. R. Brown, Handbook of Polymer Testing: Short Term Mechanical Tests (**2002**).
17. Sui, G.; Zhong, W. H.; Ren, X.; Wang, X. Q.; Yang, X. P. *Mater. Chem. Phys.* **2009**, *115*, 4024.
18. Sewda, K.; Maiti, S. N. *Polym. Bull.* **2013**, *70*, 2657.
19. Kumar, S.; Satapathy, B. K.; Maiti, S. N. *Polymer. Adv. Tech.* **2013**, *24*, 511.
20. Boscoletto, A. B.; Franco, R.; Scapin, M.; Tavan, M. *Eur. Polym. J.* **1997**, *33*, 97.
21. Nielsen, L. E.; Landel, R. F. Mechanical Properties of Polymers and Composites, 2nd edn. Marcel Dekker: New York, Basel, Hongkong (**1994**).
22. Brostow, W.; Lobland, H. E. H.; Narkis, M. *Polym. Bull.* **2011**, *67*, 1697.
23. Sewda, K.; Maiti, S. N. *J. Appl. Polym. Sci.* **2009**, *112*, 1826.
24. Lim, K. L. K.; Ishak, Z. A. M.; Ishiaku, U. S.; Fuad, A. M. Y.; Yusof, A. H.; Czigany, T.; Pukanzsky, B.; Ogunniyi, D. S. *J. Appl. Polym. Sci.* **2006**, *100*, 3931.
25. Brostow, W.; Lobland, H. E. H. *J. Mater. Sci.* **2010**, *45*, 242.